Nuclear Engineering and Technology 56 (2024) 1803–1812

Contents lists available at ScienceDirect

Nuclear Engineering and Technology

journal homepage: www.elsevier.com/locate/net

Original Article

Effect of gamma irradiation on the size of cellulose nanocrystals with polyethylene glycol and sodium hydroxide/Gd_2O_3 nanocomposite as contrast agent in magnetic resonance imaging (MRI)

Fathyah Whba [a,b,*], Faizal Mohamed [b,**], Mohd Idzat Idris [b], Rawdah Whba [c,d], Noramaliza Mohd Noor [e,f]

[a] Department of Physics, Faculty of Applied Science, Taiz University, Taiz, P.O. Box 6803, Yemen
[b] Department of Applied Physics, Faculty of Science and Technology, Universiti Kebangsaan Malaysia, Bangi, Selangor, 43600, Malaysia
[c] Department of Chemistry, Faculty of Applied Science, Taiz University, Taiz, P.O. Box 6803, Yemen
[d] Department of Engineering Physics, Istanbul Medeniyet University, 34700, Istanbul, Türkiye
[e] Department of Radiology, Faculty of Medicine and Health Science, Universiti Putra Malaysia, 43400, Serdang Selangor, Malaysia
[f] Medical Physics Unit, Hospital Sultan Abdul Aziz Shah, Universiti Putra Malaysia, 43400, Serdang Selangor, Malaysia

ARTICLE INFO

Keywords:
Gadolinium oxide nanoparticles
Cellulose nanocrystals
Gamma irradiation-reduction method
Contrast agent
Nanocomposite

ABSTRACT

The attractive properties of gadolinium-based nanoparticles as a positive contrast agent for magnetic resonance imaging (MRI) have piqued the interest of both researchers and clinicians. Nonetheless, due to the biotoxicity of gadolinium (III) ions' free radicals, there is a need to address this issue. Therefore, this research aimed to develop a biocompatible, dispersible, stable, hydrophilic, and less toxic cellulose nanocrystals/gadolinium oxide nanocomposite as contrast agent properties for MRI purposes. This study aimed to synthesize gadolinium oxide nanoparticles coated with cellulose nanocrystals with polyethylene glycol and sodium hydroxide (CNCs-PEG/NaOH)/Gd_2O_3 using the gamma irradiation method to reduce the particle size. The results showed that using a gamma irradiation dose of 10 kGy, quasi-spherical morphology with a size of approximately 5.5 ± 0.65 nm could be produced. Furthermore, the cytocompatibility of (CNCs-PEG/NaOH)/Gd_2O_3 nanocomposite synthesized was assessed through MTT assay tests on Hep G2 cells, which demonstrated good cytocompatibility without any cytotoxic effects within a concentration range of (10 μg/mL −150 μg/mL) and had sufficient cellular uptake. Moreover, the T_1-weighted MRI of (CNCs-PEG/NaOH)/Gd_2O_3 nanocomposite revealed promising results as a positive contrast agent. It is envisaged that the gamma irradiation method is promising in synthesizing (CNCs-PEG/NaOH)/Gd_2O_3 nanocomposite with nanoscale for different applications, especially in the radiotherapy field.

1. Introduction

Advanced non-invasive and non-ionizing imaging techniques, such as Magnetic Resonance Imaging (MRI), have been developed to provide high-resolution images of living organisms [1–4]. To enhance magnetic sensitivity during the imaging process, various MRI contrast agents have been developed [5,6]. These MRI contrast agents can be categorized as T_1 contrast agents, also known as positive contrast agents, or T_2 contrast agents, referred to as negative contrast agents, depending on their typical contrast mechanisms. There is a strong demand for suitable T_1 contrast agents with improved MRI T_1 signal and lower cytotoxicity. Among the various T_1 contrast agents, Gadolinium oxide nanoparticles (Gd_2O_3-NPs) stand out as the most promising option due to their significant enhancement of MRI T_1 signal and lower cytotoxicity [7,8].

Gadolinium (Gd) is a frequently employed chemical compound in diagnostic imaging, with a particular emphasis on its use in MRI. As a member of the lanthanide element family, Gd possesses paramagnetic properties that render it an appealing choice for enhancing MRI images. Gd's ability to generate a bright, positive signal intensity can significantly enhance cell visibility, simplifying the tracking of cells in low-signal tissues [9–11]. However, despite the promising potential of Gd-based contrast agents, several challenges persist and require

* Corresponding author. Department of Physics, Faculty of Applied Science, Taiz University, Taiz, P.O. Box 6803, Yemen.
** Corresponding author. Department of Applied Physics, Faculty of Science and Technology, Universiti Kebangsaan Malaysia, Bangi, Selangor, 43600, Malaysia.
E-mail addresses: wfathyah@yahoo.com (F. Whba), faizalm@ukm.edu.my (F. Mohamed).

https://doi.org/10.1016/j.net.2023.12.037
Received 16 April 2023; Received in revised form 20 October 2023; Accepted 17 December 2023
Available online 28 December 2023

attention, including concerns related to their potential toxicological effects, biodistribution, and pharmacokinetics within living systems [11].

Gadolinium (Gd) is fundamentally a complex element held together by chemical bonds between a gadolinium ion (Gd^{+3}) and a carrier molecule, known as a chelating agent. Chelating agents serve the dual purpose of mitigating the toxicity of gadolinium while preserving its contrast properties. However, the quest for innovative MRI contrast agents with enhanced attributes is ongoing, driven by the concurrent need for improved imaging effectiveness and impeccable biosafety, essential for advancing their clinical utility. Consequently, the development of carriers that incorporate Gd(III)-chelates and the refinement of their structural characteristics assume a pivotal role in creating macromolecular MRI contrast agents that are both secure and highly efficient [12].

Enhancing the water solubility and colloidal stability of paramagnetic gadolinium oxide nanoparticles (Gd_2O_3-NPs) necessitates surface modification [13,14]. Coating the nanoparticles with a protective layer prevents them from aggregating, leading to improved dispersibility and stability [15]. However, it's important to note that surface modification may impede the exchange of surface protons and bulk water protons, thereby affecting the overall longitudinal relaxation. Both the total number of surface paramagnetic Gd^{3+} ions and the distance between water protons and paramagnetic centres (which are related to the thickness of the coating) influence the relaxivity of the contrast agent [16]. Therefore, to achieve a significantly enhanced T_1 relaxivity, it is imperative to develop Gd_2O_3 contrast agents with a thin coating layer following surface modification.

Previous studies [17–20] have documented the synthesis and potential of gadolinium nanoparticles coated with biocompatible materials, including dextran, chitosan, PEG, and silica, in the development of innovative MRI contrast agents. Additionally, a recent study [21] has explored the synthesis and potential of Polyaspartic acid-coated paramagnetic gadolinium oxide nanoparticles for use as MRI contrast agents. However, the research landscape concerning gadolinium nanoparticles coated with cellulose nanocrystals is notably limited, with their application as an MRI contrast agent remaining largely uncharted. Nevertheless, it has been reported that the gamma radiolytic method can be utilized to synthesize small gadolinium nanoparticles coated with chitosan [22] through a "one-pot" approach.

In this research, cellulose nanocrystals (CNCs) are employed as a surface coating due to their numerous desirable properties. CNCs, a type of cellulose-based nanomaterial, possess a range of characteristics as documented in previous studies, including biocompatibility, biodegradability, sustainability, nontoxicity, hydrophilicity, cost-effectiveness, a substantial surface area, high mechanical strength, and exceptional stiffness [23–25]. Moreover, CNCs have found wide-ranging applications across diverse fields, such as reinforcement fillers in polymer matrices, separation membranes, transparent barrier films, supercapacitors, biomedicine, drug delivery systems, tissue engineering, and biosensors, thanks to their exceptional properties [26–28].

Furthermore, cellulose nanocrystals, derived from renewable sources like plant materials, have emerged as highly promising nanomaterials due to their innate biodegradability, low toxicity, and impressive aspect ratio. The surface chemistry and morphology of CNCs can be tailored to suit specific applications through surface modification [29]. The incorporation of polyethylene glycol (PEG), a hydrophilic polymer, can enhance the stability of CNCs dispersions, bolster their biocompatibility, and improve the imaging performance of the contrast agent. By improving dispersion, biodistribution, and clearance properties, PEG contributes to the acquisition of high-quality MRI images while minimizing potential adverse effects. The use of PEG is a strategic decision that aligns with the goal of developing safe and effective contrast agents for medical imaging applications. PEG is employed to modify the surface properties of nanoparticles, thereby enhancing their behaviour in biological systems, which has significant implications for circulation time, biodistribution, immunogenicity, and cellular interactions. The specific choice of PEG and its effects depend on the intended application of the nanoparticles, and researchers meticulously design PEG strategies to optimize the outcomes of their studies [30].

Biocompatibility characteristics assess how materials interact with biological systems without causing harm, as determined through both in vitro and in vivo evaluations. The behaviour of a material and its interaction with biology are significantly influenced by physicochemical features, which encompass factors such as particle dimensions, surface charge, and solubility. Improving these attributes leads to enhanced biocompatibility and reduced cytotoxicity. A reduction of more than 30 % in cell viability indicates cytotoxic effects. Therefore, understanding and optimizing the physicochemical properties of materials, such as $Gd2O_3$-NPs, holds critical importance in enhancing their biocompatibility and ensuring their safe and efficient integration into biomedical applications [11].

In contemporary times, Cobalt-60 stands out as a prevalent radioactive isotope frequently employed for various applications. Isotopes emitting gamma rays are considered ideal radiation sources due to their capacity to penetrate more than 1 cm into liquids or solids. Gamma rays possess a shorter wavelength compared to X-rays, resulting in higher energy per photon. Unlike X-rays, gamma radiation is typically generated from radioisotopes. Facilities utilizing gamma radiation can be employed for acute or semi-acute exposures, akin to X-ray machines. Cobalt-60 and Cesium-137 are commonly selected as sources of gamma rays in mutation breeding. When not in use, these sources are securely stored in lead containers and operated via remote control mechanisms to irradiate materials [31].

Furthermore, it has been demonstrated that gamma radiation can be employed in post-nanoparticle synthesis, particularly in the case of gold nanoparticles, to reduce their size and enhance their uniformity [32]. This method has effectively minimized the size of synthesized nanoparticles, which bear similarities to gadolinium nanoparticles as they are also metal-based. The size reduction is achieved through the radiolytic reduction of metal nanoparticles, using the reducing species generated by water radiolysis, known as radicals. Despite the potential of radiation in reducing the size of gadolinium-based nanoparticles after synthesis, there is a noticeable dearth of studies conducted on this particular subject.

Therefore, the focus of this study is to investigate the impact of gamma irradiation on cellulose nanocrystals/Gd_2O_3 nanocomposite as a contrast agent for magnetic resonance imaging (MRI). It should be noted that the gadolinium nanoparticles were synthesized using the sol-gel method and then coated with cellulose nanocrystals with polyethylene glycol and sodium hydroxide to form a biocompatible, stable, and hydrophilic substrate. The resulting nanocomposite is obtained by loading magnetic Gd_2O_3 nanoparticles onto the CNCs-PEG/NaOH nanoplatform. Additionally, gamma radiation is used after the synthesis of the nanocomposite to decrease their size and increase their uniformity. The aim of this study is to utilize gamma irradiation to reduce the size of nanoparticles, enhance their uniformity after synthesis and explore their potential as contrast agents for MRI.

2. Experimental

2.1. Materials

All chemicals, including Gadolinium chloride hexahydrate ($GdCl_3{\cdot}6H_2O$) (99.9 %, M_w = 371.70 g mol^{-1}), Sodium hydroxide (NaOH) (>99.9 %, M_w = 40 g $mol^{-}1$), ethylene glycol ($C_2H_6O_2$) (99 %, M_w = 62.97 g mol^{-1}), polyethylene glycol ($C_{2n}H_{4n}+2O_{n+1}$) (99 %, M_w = 6000 g mol^{-1}), microcrystalline cellulose $(C_6H_{10}O_5)_n$ (99 %, M_w = 370.35 g mol^{-1}), sulfuric acid (H_2SO_4) (99.9 %, M_w = 98.080 g mol^{-1}), were procured from Sigma-Aldrich and utilized without the need for further purification. Ethanol (C_2H_6O) (99 %, M_w = 46.07 g mol^{-1}, HmbG® chemicals) was employed for the initial washing of the

nanoparticles. Distilled water, filtered by Purelab Maxima ELGA, with a resistivity value of 18.2 MΩ, was used for the final washing of the nanoparticles.

2.2. Method

2.2.1. Synthesis of gadolinium oxide (Gd_2O_3) nanoparticles

Gadolinium oxide nanoparticles (Gd_2O_3-NPs) were synthesized via the sol-gel method, in accordance with our previously reported work [11,33]. Whereby an adequate production of nanoparticles with a high yield and purity percentage was achieved at certain annealing temperatures without the additional use of a catalyst agent. In brief, EG was used as $GdCl_3.6H_2O$ dissolving agent and NaOH as precipitation facilitating agent. Formed gadolinium hydroxide ($GdOH_3$) powder was then annealed at various temperatures (500 °C–1100 °C) for 3 h with a heating rate of 5 °C/min to facilitate spontaneous decomposition of Gd $(OH)_3$. Thus, the dehydration process yields Gd_2O_3 nanopowder of crystalline structure.

2.2.2. Preparation of cellulose nanocrystals (CNCs) via sulfuric acid hydrolysis

As per our previous work [30], the synthesis of cellulose nanocrystals (CNCs) through acid hydrolysis follows a controlled chemical hydrolysis reaction, as depicted in (Fig. A1) and described by Ref. [34]. The acid hydrolysis method was chosen for generating CNCs from commercially sourced microcrystalline cellulose (MCC) due to its anticipated high yield, resulting in a stable aqueous suspension with a high crystallinity index. In brief, 14 mmol of MCC was dispersed in 100 mL of distilled water and stirred at room temperature for 1 h. Separately, 64 % (v/v) sulfuric acid (H_2SO_4) was dissolved in 36 mL of distilled water and stirred for 10 min at room temperature. Subsequently, 50 mL of the acid solution was slowly added to the MCC suspension to achieve a pH of approximately 0.82. The mixed solution was heated with constant mechanical stirring at 45 °C for an hour. After this, 200 mL of cold distilled water was added to halt the hydrolysis reaction. The resulting CNCs, appearing white, were collected by centrifugation at 4020 rpm for 20 min. The product underwent multiple washes by vortexing in distilled water at 2200 rpm for 2 min, followed by centrifugation at 4020 rpm for 20 min to remove unreacted precursors, i.e., sulfate ions. This washing step was repeated until the pH of the product reached approximately 6–7. The final CNCs product was freeze-dried at 45 °C for 24 h and then ground into a powder using a crucible. Eq. (1), as proposed by Sfiligoj et al. (2019) [35], was used to estimate the yield percentage (%Y) of the prepared sample (Table S1). A photograph of the synthesized cellulose nanocrystals (CNCs) is shown in (Fig. A2).

$$\%\ Yield = \frac{Weight\ after\ hydrolysis}{Weight\ intial} X\ 100\ \% \quad (1)$$

2.2.3. Synthesis of (CNCs-PEG/NaOH) via hydrolysis method

As detailed in our prior work [30], the hydrolysis method was employed to produce cellulose nanocrystals (CNCs) with PEG/NaOH. This method was chosen for its capacity to generate a stable aqueous suspension of CNCs with a high crystallinity index. To execute the procedure, 4 g of polyethylene glycol (PEG) with a molecular weight of 6000 g/mol was dissolved in 100 mL of distilled water and stirred for 10 min at room temperature. In a separate step, 8 g of sodium hydroxide (NaOH) was dissolved in 100 mL of distilled water and stirred for 10 min at room temperature. Subsequently, 20 mL of the previously prepared PEG solution was slowly added to the 80 mL of NaOH solution while stirring for 10 min at room temperature. A 0.5 % w/v solution of CNCs was prepared by mixing 0.5 g of CNCs in 100 mL of the PEG/NaOH solution. After a week of stirring, the mixture was subjected to centrifugation at 4020 rpm for 20 min. The resulting white product, referred to as (CNCs-PEG/NaOH), was collected and further dried using freeze-drying at 45 °C for 24 h. The dried product was stored at 4 °C until further use. Eq. (1), as proposed by Sfiligoj et al. (2019) [35], was used to estimate the yield percentage (%Y) of the prepared sample (Table A1). The final synthesized (CNCs-PEG/NaOH) is depicted in (Fig. A3).

2.2.4. Synthesis of (CNCs-PEG/NaOH)/Gd_2O_3 through gamma-ray irradiation

A solution of cellulose nanocrystals with PEG/NaOH, containing 0.5 % w/v of CNCs, was mixed with 40 mL of Gd_2O_3 solution in acetic acid (2 % v/v) at 1000 °C and 0.1 mmol of synthesized Gd_2O_3-NPs. After stirring the mixture for seven days at room temperature, it was subjected to gamma irradiation at Universiti Kebangsaan Malaysia using a cobalt-60 Gammacell Excel Nordion 200 irradiator. The gamma irradiation dose was varied at 3 kGy, 8 kGy, 10 kGy, 30 kGy, and 40 kGy, with a dose rate of 12 kGy/h, to create the nanocomposite of gadolinium oxide nanoparticles coated with cellulose nanocrystals (CNCs-PEG/NaOH)/Gd_2O_3. A solution of nanoclusters was prepared following the same procedure but without the inclusion of Gd_2O_3, which was used as a control. A schematic depiction of synthesized (CNCs-PEG/NaOH)/Gd_2O_3 nanocomposite through gamma-ray irradiation is shown in Fig. 1.

2.3. Characterization

Molecular weight analysis was performed using the Gel Permeation Chromatography (GPC) method with a Waters 2414 system equipped with a Styragel® column and a differential refractive index (2414) detector. A 1 mg sample was dissolved in 1 mL of tetrahydrofuran (THF) using a flow rate of 1 mL/min at a temperature of 30 °C. To confirm the chemical interaction between cellulose nanocrystals with polyethylene glycol and sodium hydroxide and to identify the sample structures, ^1H and ^{13}C nuclear magnetic resonance (NMR) spectra were recorded using a Bruker/Advance III HD 400 MHz spectrometer (Bruker, Rheinstetten, Germany). However, solid-state NMR spectroscopy was not available at the Centre of Research and Instrumentation Management, Universiti Kebangsaan Malaysia. As a substitute, the CNCs-PEG/NaOH (30 mg) sample was dissolved in Deuterium oxide (D_2O, 0.6 mL) for 3 h at room temperature. The average particle diameter was determined through transmission electron microscopy (Phillips CM12) at an accelerating voltage of 120 kV. For TEM analysis, a small amount (<1 mg) of the sample was suspended in ethanol, sonicated for 15 min, and then deposited onto a TEM grid. The solution was subsequently air-dried at room temperature before characterization. The size of the sample suspensions was estimated using Dynamic Light Scattering (DLS) with a Malvern 3000 Zetasizer Nano ZS instrument, using a detection angle of 173° and a wavelength of 633 nm at room temperature. To ensure good dispersion, a small quantity of the sample was dissolved in deionized water and sonicated. The hydrodynamic size measurements were obtained after maintaining the samples at a consistent temperature of 25 °C for 2 min. Meanwhile, the experiment involved subjecting (CNCs-PEG/NaOH)/Gd_2O_3 nanocomposite solutions to gamma radiation using the MDS Nordion Gammacell 220 Excel irradiator at dosage levels ranging from 0 to 40 kGy. The gamma cells had an uncertainty of ±2.7 % at a 95 % confidence level, and the estimated dose rate was approximately 4.20 kGy/h.

2.4. In vitro MRI studies

To evaluate the effectiveness of the (CNCs-PEG/NaOH)/Gd_2O_3 nanocomposite as an MRI contrast agent, an experimental setup was utilized. Initially, a phantom was created by introducing the synthesized (CNCs-PEG/NaOH)/Gd_2O_3 nanocomposite into Petri dishes, filling them with a 15 mL volume. These Petri dishes were then placed within a phantom containing tap water, which ensured optimal image acquisition [36]. The constructed phantom was positioned at the isocenter of a magnetic resonance imaging (MRI) system with a 3.0 T field strength (Siemens Magnetom Verio, National Cancer Institute). Imaging was

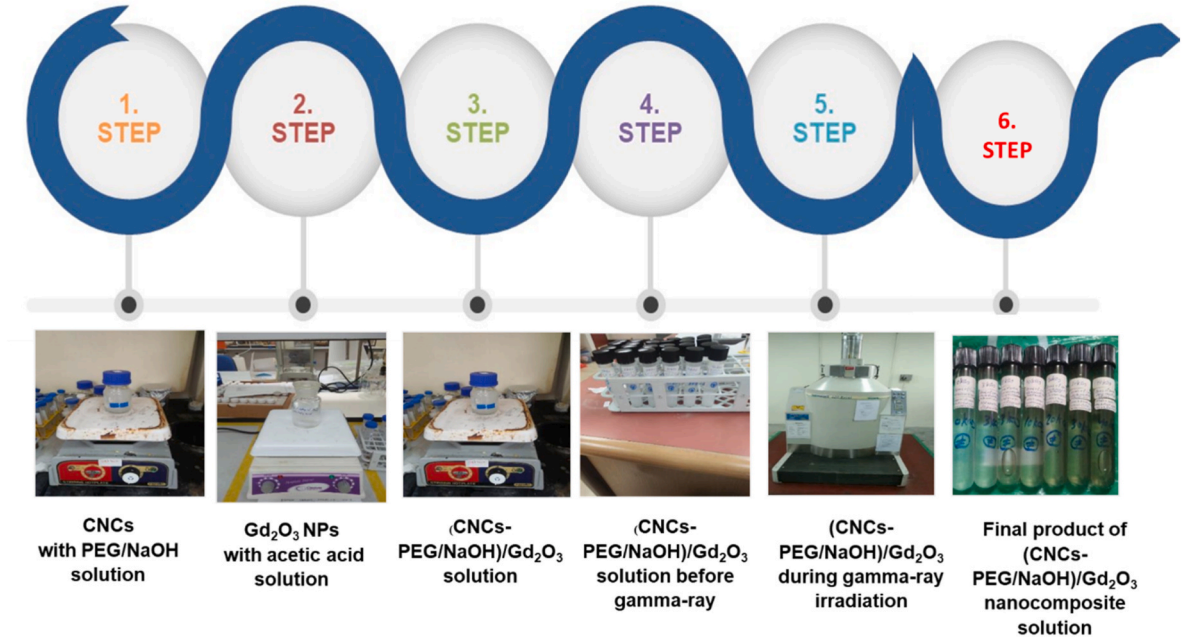

Fig. 1. Schematic representation of synthesized (CNC-PEG/NaOH)/Gd_2O_3 through gamma-ray irradiation.

conducted using the MR coil head. For T_1-weighted imaging, the parameters employed were as follows: field of view (FOV) = 179 mm × 220 mm, echo time (TE) = 10 ms, and repetition time (TR) = 2220 ms. Additionally, T_2-weighted images were also obtained with a TR value of 3000 ms and TE = 10 ms. The acquired MR images were subsequently analyzed, with a focus on assessing the quality of the achieved contrast. This qualitative evaluation aimed to determine the potential suitability of the synthesized (CNCs-PEG/NaOH)/Gd_2O_3 nanocomposite as an effective MRI contrast agent.

3. Results and discussion

3.1. Molecular weight distribution (MWD) analysis

Molecular weight distribution (MWD) measurements were conducted using gel permeation chromatography (GPC) to determine the weight average molecular weight (M_w), number of average molecular weight (M_n), and the polydispersity index (PDI) of cellulose nanocrystals with polyethylene glycol and sodium hydroxide (CNCs-PEG/NaOH). Table 1 illustrates that Mw is greater than Mn because larger molecules contain more mass than smaller ones. Consequently, the contribution of more substantial molecules to the molecular weight average holds more significance.

Furthermore, the polydispersity index (PDI), which represents the ratio of Mw to Mn, serves as an indicator of the sample's uniformity. As reported by Potthast et al. (2015) [37], a PDI value approaching 1 indicates a sample with a narrow molecular weight distribution (MWD), reflecting uniformity, while higher values signify increased non-uniformity. In terms of PDI, the CNCs-PEG/NaOH exhibits a value of 1.14, indicating that the mixture is uniform and possesses a narrow MWD. These findings align with previous reports [38] on the uniformity of CNCs-PEG/NaOH.

Table 1
The gel permeation chromatography data of (CNCs-PEG/NaOH).

Sample ID	Number average molecular weight (M_n) (g mole^{-1})	Average molecular weight (M_w) (g mole^{-1})	Polydispersity index (PDI) (M_w/M_n)
CNCs-PEG/NaOH	74 766	85 915	1.14

3.2. Nuclear magnetic resonance (NMR) analysis

Polyethylene glycol (PEG), cellulose nanocrystals (CNCs), and the cellulose solution in the aqueous PEG/NaOH mixture (CNCs-PEG/NaOH) were analyzed using proton and carbon nuclear magnetic resonances (^{1}H NMR and ^{13}C NMR). The results of the analysis are presented in Figs. 2 and 3. Fig. 2(c) displays the ^{1}H NMR spectrum of CNCs-PEG/NaOH (400 MHz, D_2O, δ (ppm)). CNCs-PEG/NaOH exhibited signals consistent with previous studies [38] for the protons of (−$CH^a_2CH_2O$), the methylene group (−CH^c_2O), (HO–CH^d_2), and the D_2O solvent residue, with chemical shifts of δ 2.4 ppm, δ 3.64 ppm, δ 3.4 ppm, and δ 4.71 ppm, respectively (as shown in Fig. 2(b) and (c)). Notably, new peaks were observed in the CNCs-PEG/NaOH sample: δ 1.85 ppm (peak b) for the methyl proton (−CH_3) from the CNCs chain and δ 8.39 ppm (peak e), possibly corresponding to the –OH of alcohol oxidized into an aldehyde group.

Fig. 3(b) illustrates the NMR spectrum of CNCs, revealing characteristic peaks of cellulose. The peak in the chemical shift range of 62–66 ppm is associated with carbon C^6 and indicative of amorphous cellulose. The peak at a chemical shift of 104–107 ppm corresponds to carbon C^1. The chemical shift range of 82–90 ppm is attributed to carbon C^4, with a value of 84 ppm for amorphous cellulose chains and 89 ppm for crystalline chains. The carbons C^2, C^3, and C^5 are represented by the region between 71 and 77 ppm. These carbon atoms are not involved in the β (1–4) linkage and could not be distinguished. These signals align with previous studies on cellulose [39–42].

Furthermore, as per our previous work [30], the ^{13}C NMR spectra of the cellulose solution at room temperature exhibited similar signals to the CNCs sample, with slight variations in intensity (Fig. 3(c)). Notably, new peaks (*) were observed at 52 ppm, 63 ppm, 69.9 ppm, and 89 ppm, characteristic of PEG chains (as shown in Fig. 3(a)), consistent with prior studies [43,44]. The change in the position of C^4 suggested a disruption of hydrogen bonds within the cellulose molecule, similar to the case of wood pulp dissolved in LiCl/DMAc (as reported by McCormick et al., in 1985) [45]. Additionally, the peak at 167 ppm was attributed to C*, indicating the conversion of one hydroxyl group into a carboxyl group,

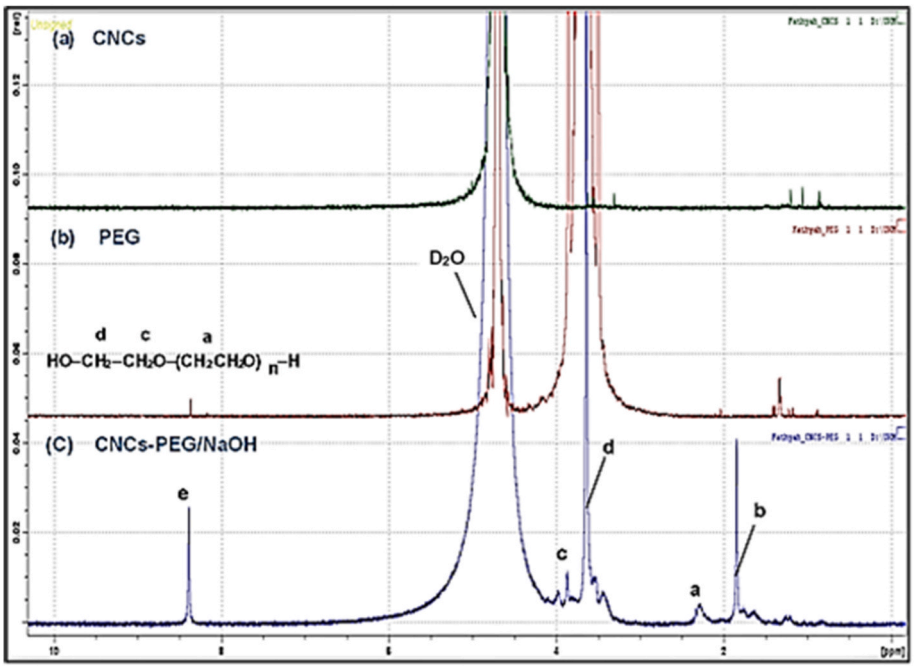

Fig. 2. ^{1}H NMR spectra of (a) CNCs, (b) PEG, (c) CNCs-PEG/NaOH solution.

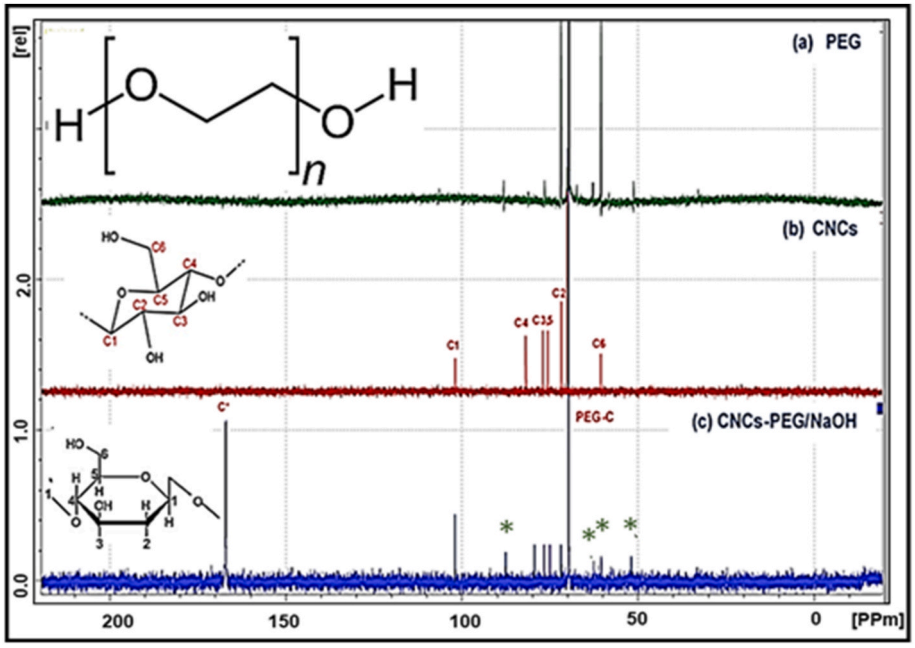

Fig. 3. ^{13}C NMR spectra of (a) PEG, (b) CNCs, (c) CNCs-PEG/NaOH solution.

in line with the results reported by Ref. [38].

3.3. Characterization using transmission electron microscope (TEM)

Ensuring the size distribution of metallic nanoparticles is well-controlled is a crucial aspect of their preparation. To address this concern, the morphology and size of nanocomposite particles produced using the gamma irradiation method were examined through TEM. The TEM micrographs obtained revealed that all (CNCs-PEG/NaOH)/Gd_2O_3 nanocomposite samples exhibited a spherical shape with a core-shell structure. The particle size was notably influenced by the gamma irradiation dose, as demonstrated in Fig. 4. Furthermore, with varying irradiation doses, the (CNCs-PEG/NaOH)/Gd_2O_3 nanocomposite displayed a reduction in the average particle size alongside a change in its shape. It's worth highlighting that the (CNCs-PEG/NaOH)/Gd_2O_3 nanocomposite subjected to a dose of 10 kGy exhibited a smaller particle size compared to other dosages, which aligns with the results reported by Ref. [46].

3.4. Dynamic Light Scattering (DLS) analysis

Dynamic Light Scattering (DLS) was performed to examine the particle size distribution of the (CNCs-PEG/NaOH)/Gd_2O_3 nanocomposite after irradiation at different doses, providing additional data to support

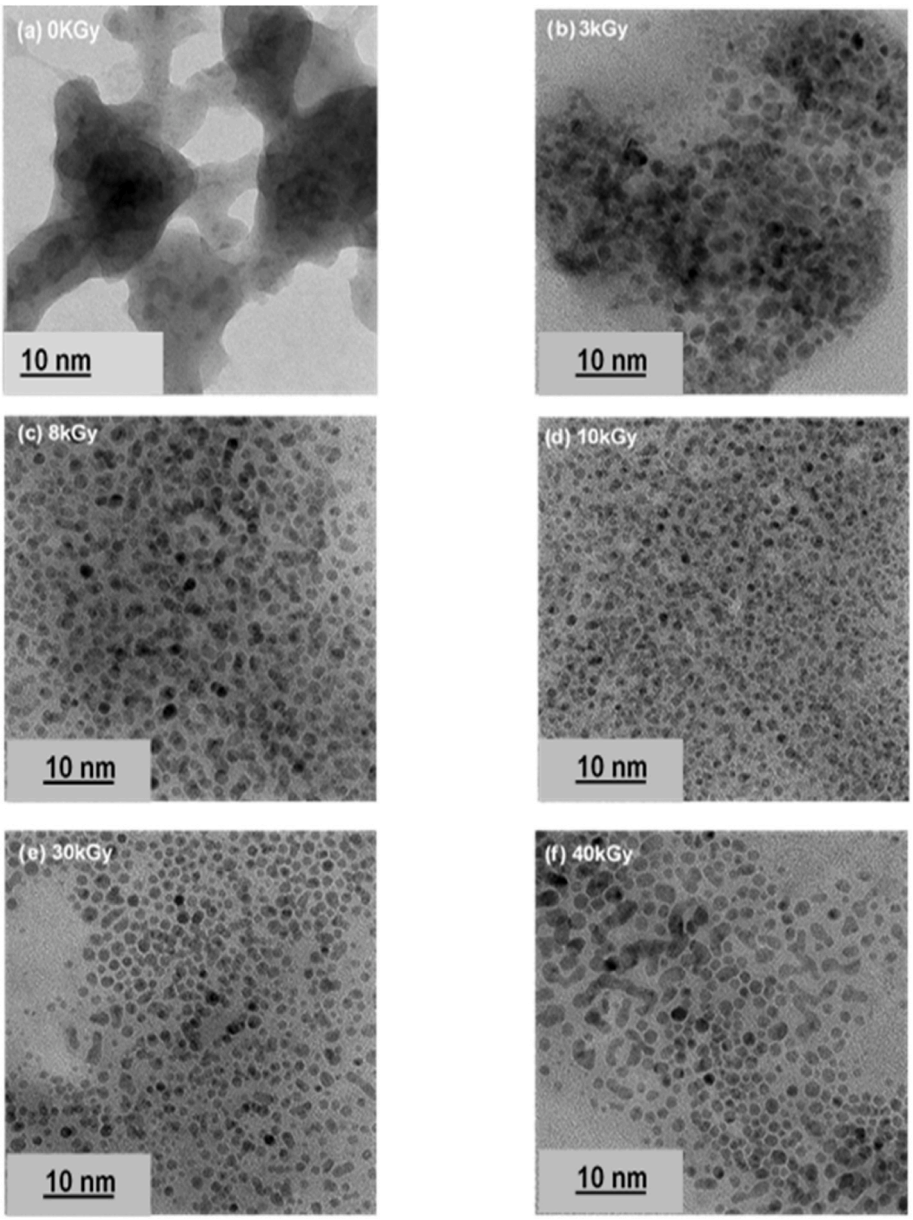

Fig. 4. TEM micrographs of nanocomposite at different doses (a) 0 kGy (b) 3 kGy, (c) 8 kGy, (d) 10 kGy, (e) 30 kGy and (f) 40 kGy.

the particle size information obtained from TEM images.

Fig. 5 reveals that the (CNCs-PEG/NaOH)/Gd_2O_3 nanocomposite exposed to a dose of 10 kGy displayed a smaller average size of 5.5 ± 0.65 nm, with a polydispersity index (PDI) of 1.0. This finding confirms that the average size of the (CNCs-PEG/NaOH)/Gd_2O_3 nanocomposite at 10 kGy is the smallest (Fig. 4) compared to doses of 0 kGy, 3 kGy, 8 kGy, 30 kGy, and 40 kGy after irradiation.

To explore the impact of gamma-ray dose on particle size, the particles were measured and graphed against the dose, and the size distribution of the (CNCs-PEG/NaOH)/Gd_2O_3 nanocomposite is presented in Fig. 6. The graph illustrates that the particle size of the (CNCs-PEG/NaOH)/Gd_2O_3 nanocomposite is influenced by the gamma-ray dose. As the dose increased from 0 kGy to 10 kGy, the average particle size of the (CNCs-PEG/NaOH)/Gd_2O_3 nanocomposite decreased significantly from 25.39 ± 3.021 nm to 5.5 ± 0.65 nm. This decrease can be attributed to the diverse effects of gamma irradiation on nanomaterials, including chain scission and crosslinking. At doses below 10 kGy, irradiation mainly leads to the cleavage of polymer chains (such as cellulose and PEG), resulting in smaller fragments or nanoparticles and a reduction in particle size. Furthermore, irradiation can alter nanoparticle surface chemistry and interactions, which can disperse fragments and cause size reduction due to changes in surface properties.

The results indicate that the particle size of the (CNCs-PEG/NaOH)/Gd_2O_3 nanocomposite remains almost constant at radiation doses of 8 kGy and 10 kGy, measuring at 6.371 ± 1.35 nm and 5.5 ± 0.65 nm, respectively. However, at higher doses of 40 kGy, the (CNCs-PEG/NaOH)/Gd_2O_3 nanocomposite undergoes degradation and denaturation. It is important to note that the particle size of the (CNCs-PEG/NaOH)/Gd_2O_3 nanocomposite increased to 8.021 ± 2.01 nm and 9.5 ± 1.17 nm after gamma irradiation at doses of 30 kGy and 40 kGy. This increase is attributed to the fact that higher doses can lead to the recombination of cleavage products through crosslinking or radiation-driven chemistry, potentially resulting in larger particle sizes. Additionally, higher doses may foster aggregation or growth due to modified surface properties. These findings confirm that gamma irradiation can produce nanoparticles within the nanoscale range for (CNCs-PEG/NaOH)/Gd_2O_3, consistent with previous reports by Ref. [46].

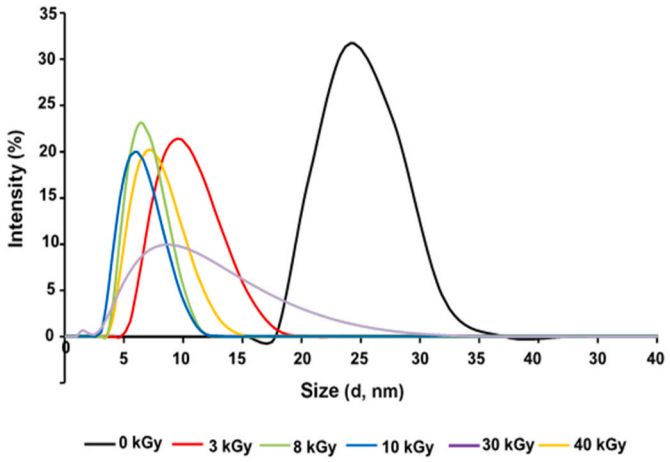

Fig. 5. DLS spectra of (CNCs-PEG/NaOH)/Gd_2O_3 nanocomposite at different doses.

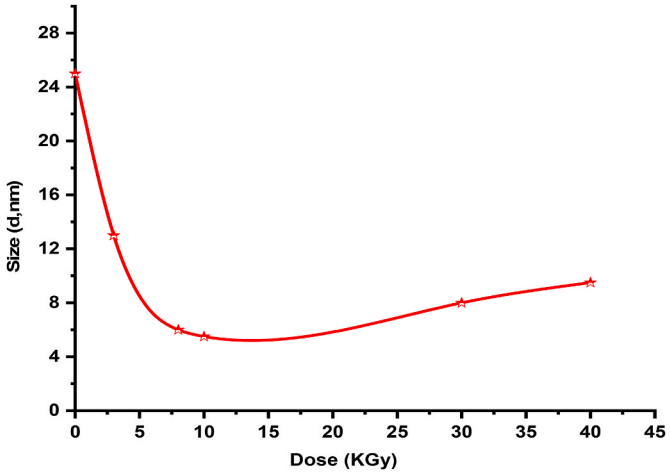

Fig. 6. Particle size distribution post gamma irradiation at different doses (0 kGy-40 kGy).

3.5. *Effects of Concentration of (CNCs-PEG/NaOH)/Gd_2O_3 nanocomposite (10 kGy) on Hep G2 cells*

The cytotoxicity test is a vital method for evaluating cell health and determining whether a substance is toxic to cells or not. Cell death can occur through two main mechanisms: necrosis and apoptosis. Necrosis typically results from cell injury, while apoptosis is a regulated process of cell death common in multicellular organisms [47]. Apoptosis can be triggered by various external factors such as infection, toxicity, or trauma, leading to the controlled breakdown of cell components.

Given the potential utility of Gd nanoparticles as contrast agents to enhance MRI image quality, a study was conducted to assess their impact on biological cells. In this phase, the test material, (CNCs-PEG/NaOH)/Gd_2O_3 nanocomposite (10 kGy), was selected for evaluating cell survival, following ISO 10993–5:2009 guidelines. The MTT assay [48,49] was used to assess cell viability through colourimetric analysis. Lower optical density (OD) readings are indicative of reduced cell survival, suggesting a loss of mitochondrial dehydrogenase activity. The positive control for this test involved using hydrogen peroxide (H_2O_2) (10 mM), and the control medium was the complete growth medium. The formation of formazan in Hep G2 cells due to mitochondrial reductase activity in response to the positive control H_2O_2 is illustrated in Fig. 7.

Fig. 8 shows the percentage of cell survival on Hep G2 cells at a

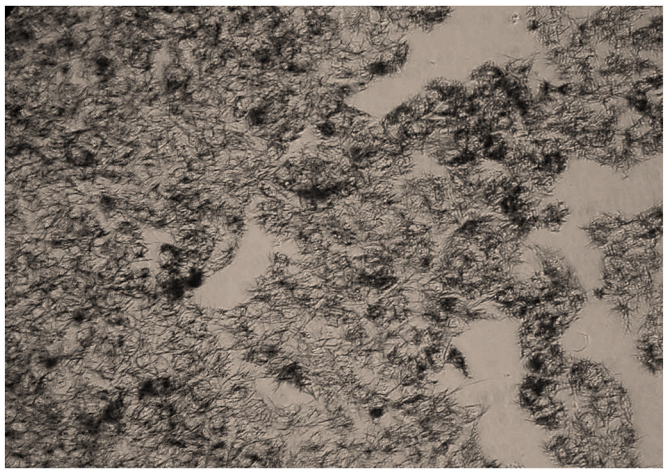

Fig. 7. Microscopic examination of Hep G2 cells in the presence of H_2O_2 as a positive control shows a decrease in MTT occurring on Hep G2 cells.

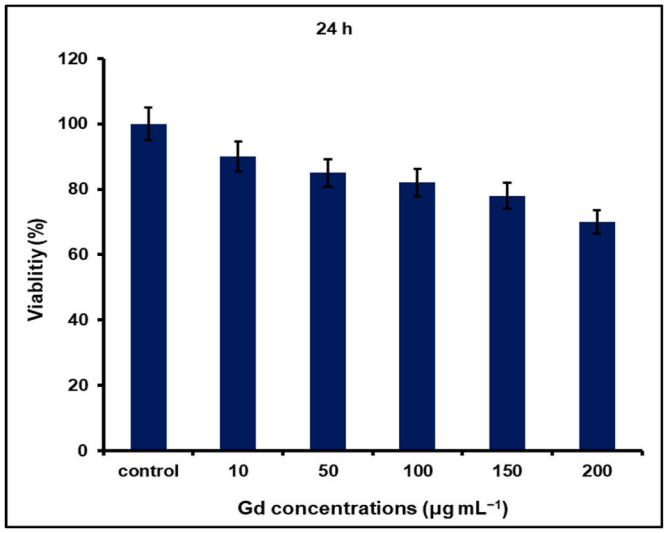

Fig. 8. Effect of (CNCs-PEG/NaOH)/Gd_2O_3 nanocomposite on the survival of Hep G2cells. Cell survival was treated with a concentration range of 10 μg/mL–200 μg/mL after irradiated at 10 kGy.

seeding density of 20 000 cells/well after incubation with (CNCs-PEG/NaOH)/Gd_2O_3 nanocomposite at different Gd concentrations (10 μg/mL, 50 μg/mL, 100 μg/mL, 150 μg/mL and 200 μg/mL) [50] for 24 h at 37 °C in a humidified atmosphere consisting of 5 % carbon dioxide and 95 % air. In addition, if we look at the (CNCs-PEG/NaOH)/Gd_2O_3 nanocomposite sample, the survival of Hep G2 cells is decreasing and it is directly proportional to the increase in the concentration of (CNCs-PEG/NaOH)/Gd_2O_3 nanocomposite in the range of 10 μg/mL-200 μg/mL. Due to the presence of 2 % v/v acetic acid to form a gadolinium oxide solution. The presence of acid in HepG2 cells is one of the factors that cause cell survival to decrease. Nevertheless, despite the presence of acetic acid in the (CNCs-PEG/NaOH)/Gd_2O_3 nanocomposite sample, it did not show a cytotoxic effect on Hep G2 cells. These findings are consistent with previous reports by Ref. [11].

Moreover, the survival of Hep G2 cells in the (CNCs-PEG/NaOH)/Gd_2O_3 nanocomposite sample at a concentration of 200 μg/mL showed over 50 % cell survival (70 ± 2), albeit less than the control cells, as demonstrated in Fig. 8 and Table 2. In accordance with the ISO guidance, if the survival of Hep G2 cells signal is reduced to <70 % of the blank control, the sample is considered potentially cytotoxic.

As per a study by Refs. [51,52], both the pH value and the

Table 2
Hep G2 cell viability was obtained after 24 h of (CNCs-PEG/NaOH)/Gd_2O_3 nanocomposite after irradiated at 10 kGy with hydrogen peroxide (H_2O_2) as positive control.

Viability (%)	Replicate	Positive control (10 mM)	Negative control	(CNCs-PEG/NaOH)/Gd_2O_3nanocomposite (μg/mL)				
				10	50	100	150	200
	n = 1	12	100	89	83	81	79	68
	n = 2		100	89	86	80	79	69
	n = 3		100	91	87	84	74	72
	Mean	NA	100	90	85	82	78	70
	Standard Error Mean	NA	0	1	2	2	3	2

concentration of the test substance can influence the formation of MTT-formazan in the culture medium. In this study, a reduction in cell survival exceeding 30 % was considered indicative of cytotoxicity [53]. The findings unequivocally indicate that the (CNCs-PEG/NaOH)/Gd_2O_3 nanocomposite, exhibited good cytocompatibility. It showed no cytotoxic effects on Hep G2 cells within a concentration range of 10 μg/mL to 150 μg/mL, underscoring its suitability as an MR imaging contrast agent.

3.6. Cellular uptake in vitro

The investigation of biological applications of nanoparticles involves an examination of their ability to enter cells. In this study, the cellular uptake of (CNCs-PEG/NaOH)/Gd_2O_3 nanocomposites after irradiation at 10 kGy was assessed by incubating Hep G2 cells with varying concentrations of the nanocomposite. After 6 h, the content of gadolinium within the cells was quantified using ICP-MS (see Table A2). Moreover, the cell viability, cell concentration, and the total number of cells in the original sample (6 mL) were determined through the methods outlined in (Method A1). The results indicated that cell viability, cell concentration, and the total number of cells were 98.2 %, 22.4 cells/mL, and 134.4 cells, respectively.

Fig. 9 illustrates the relationship between the Gd concentration (pg/cell) within the cells and the Gd concentration (μg mL^{-1}) in the (CNCs-PEG/NaOH)/Gd_2O_3 solution used during the incubation process. The data shows that cellular uptake of Gd increased as the concentration of (CNCs-PEG/NaOH)/Gd_2O_3 nanocomposite in the solution increased over a specific time. The findings indicated that the nanocomposite demonstrated sufficient cellular uptake, which has the potential to enhance MRI contrast. This uptake can be attributed to the fact that intracellular absorption is influenced by particle size and shape, with smaller particles having a tendency for higher intracellular uptake compared to larger ones, as previously reported by Suryani and Ismail (2015) [54].

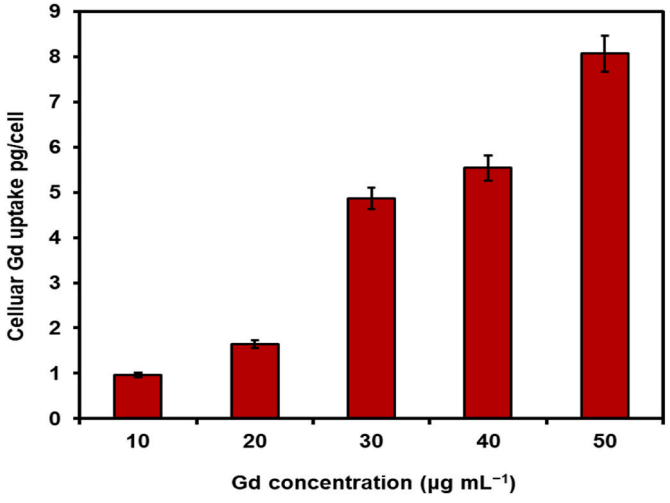

Fig. 9. Hep G2 cell uptake of different gadolinium concentrations of nanocomposite for 6 h after irradiated at 10 kGy.

3.7. T1- weighted and T2-Weighted MR images

Based on the results displayed in Fig. 10(a), it is evident that the synthesized (CNCs-PEG/NaOH)/Gd_2O_3 nanocomposite serves as an effective contrast agent, producing bright images in contrast to the water background. This demonstrates its capability to enhance T_1 relaxation, resulting in increased signal intensity on T_1-weighted images. Additionally, it was observed, as shown in Fig. 10, that the T_1-weighted image signal intensity of the nanocomposite at 30 kGy (Fig. 10 (5)) is stronger than that at 40 kGy (Fig. 10(6)). This variation can be attributed to changes in tissue structure or the contrast agent itself, which can modify their interaction with the magnetic field, subsequently influencing signal intensity. Alterations in molecular conformation, aggregation, or mobility can impact the T_1 relaxation properties, leading to increased signal intensity. The different radiation doses may influence water dynamics differently, resulting in the observed variations in signal intensity [11].

Despite the fact that the T_2 image in Fig. 10(b) did not reveal significant changes in all specimens following irradiation at 0 kGy, 3 kGy, 8 kGy, 10 kGy, 30 kGy, and 40 kGy, TEM images showed that the nanoparticles were smaller in size at a dose of 10 kGy. The reduction in nanoparticle size may facilitate the elimination of Gd ions through the excretory system, indirectly reducing the duration of Gd's presence in the body. Additionally, nanoparticle size can affect their circulation time, biodistribution, and cellular uptake. Smaller nanoparticles can more easily enter cells, which can be advantageous for intracellular drug delivery. Moreover, smaller nanocomposites usually exhibit shorter T_2 relaxation times due to their increased susceptibility to magnetic field in homogeneities. Shorter T_2 relaxation times can lead to more efficient suppression of unwanted signals from surrounding tissues in T_2-weighted imaging.

Furthermore, smaller nanocomposites typically have a higher surface area-to-volume ratio, enabling them to interact more readily with the surrounding tissues. Consequently, they may accumulate in the target area more quickly, reducing the time required for imaging, as the contrast agent becomes effective sooner. In contrast, larger nanocomposites may take longer to accumulate in target tissues due to their reduced mobility and slower diffusion. As a result, the imaging time might need to be extended to allow sufficient accumulation for adequate contrast enhancement. Therefore, the choice of nanocomposite size should align with the specific clinical application. For instance, in cancer imaging, smaller nanocomposites may be preferred for detecting small lesions, while larger ones might be more suitable for vascular imaging or organ-specific applications.

Consistently, the gamma irradiation reduction method can be utilized to control nanoparticle size and holds significant potential for various applications involving gadolinium nanoparticles.

4. Conclusions

The potential of (CNCs-PEG/NaOH)/Gd_2O_3 as a contrast agent in

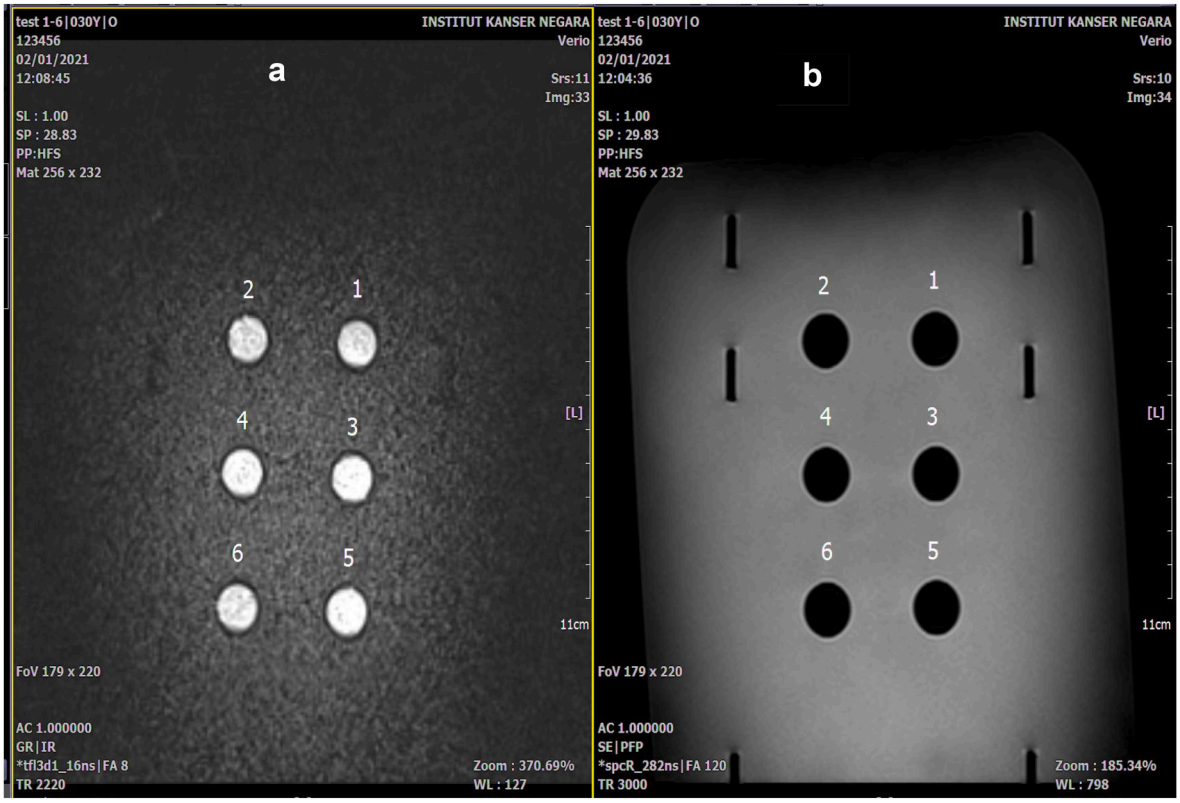

Fig. 10. T_1 and T_2-weighted images of nanocomposite at different doses (1) 0 kGy (2) 3 kGy, (3) 8 kGy, (4) 10 kGy, (5) 30 kGy and (6) 40 kGy.

MRI phantoms was investigated to evaluate the impact of different doses on image weighting. It can be concluded that contrast media in a solid-state form are not suitable for use in the human body compared to their liquid state counterparts due to their homogeneous nature. While the T^1-weighted images did not exhibit significant changes in all the samples after irradiation at doses of 3 kGy, 8 kGy, 10 kGy, 30 kGy, and 40 kGy, TEM images revealed that the particle size was reduced at the 10 kGy dose. The smaller size of the particles facilitates the removal of Gd ions through the excretory system, indirectly reducing the duration of Gd's presence in the body. This study suggests that this method can be employed to control the size of metal particles and holds potential applications in various fields related to gadolinium nanoparticles. In conclusion, gadolinium exhibits considerable promise as it can address both the requirements of intelligent delivery for high-quality MRI imaging in the biomedical field. However, further improvements in magnetic properties are required to develop a dual contrast composite material for different applications, especially in the radiotherapy field.

Declaration of competing interests

The authors declare that they have no known competing financial interests or personal relationships that could have appeared to influence the work reported in this paper.

Acknowledgements

The authors express their gratitude to Universiti Kebangsaan Malaysia (UKM) for their support through grants UKM-GUP-2022-046 and UKM-GUP-2020-035. They would also like to extend their appreciation to the government of Yemen, represented by the Ministry of Higher Education and Scientific Research, for their funding of the scholar project.

Appendix A. Supplementary data

Supplementary data to this article can be found online at https://doi.org/10.1016/j.net.2023.12.037.

References

[1] T.N. Turan, Z. Rumboldt, T.R. Brown, High-resolution MRI of basilar atherosclerosis: three-dimensional acquisition and FLAIR sequences, Brain Behav. 3 (2013) 1–3.
[2] P.C. Wu, C.H. Su, F.Y. Cheng, J.C. Weng, J.H. Chen, T.L. Tsai, D.B. Shieh, Modularly assembled magnetite nanoparticles enhance in vivo targeting for magnetic resonance cancer imaging, Bioconjugate Chem. 19 (2008) 1972–1979.
[3] Y. Xiao, J. Du, Superparamagnetic nanoparticles for biomedical applications, J. Mater. Chem. B 8 (2020) 354–367. .
[4] Z. Zuo, T. Syrovets, F. Genze, A. Abaei, G. Ma, T. Simmet, V. Rasche, High-resolution MRI analysis of breast cancer xenograft on the chick chorioallantoic membrane, Nucl. Magn. Reson.Biomed. 28 (2015) 440–447.
[5] J.W. Bulte, D.L. Kraitchman, Iron oxide MR contrast agents for molecular and cellular imaging. NMR in biomedicine, Int. J.devoted Dev.Appl. Magn. Reson.In Vivo 17 (2004) 484–499.
[6] P. Caravan, Strategies for increasing the sensitivity of gadolinium based MRI contrast agents, Chem. Soc. Rev. 35 (2006) 512–523.
[7] H.B. Na, J.H. Lee, K. An, Y.I. Park, M. Park, I.S. Lee, T. Hyeon, Development of a T1 contrast agent for magnetic resonance imaging using MnO nanoparticles, Angew. Chem. 119 (2007) 5493–5497.
[8] H.B. Na, T. Hyeon, Nanostructured T1 MRI contrast agents, J. Mater. Chem. 19 (2009) 6267–6273.
[9] H. Dong, S.R. Du, X.Y.l. Zheng, G.M. Lyu, L.D. Sun, L.D. Li, P.Z. Zhang, C. Zhang, Lanthanide nanoparticles: from design toward bioimaging and therapy, Chem. Rev. 115 (2015) 10725–10815.
[10] F. Wang, E. Peng, B. Zheng, S.F.Y. Li, J.M. Xue, Synthesis of water-dispersible Gd_2O_3/GO nanocomposites with enhanced MRI T_1 relaxivity, J. Phys. Chem. C 119 (2015) 23735–23742.
[11] F. Whba, F. Mohamed, M.I. Idris, Evaluation of physicochemical and biocompatibility characteristics of gadolinium oxide nanoparticles as magnetic resonance imaging contrast agents, Radiat. Phys. Chem. 213 (2023), 111189.
[12] C. Guo, L. Sun, H. Cai, Duan, S. Zhang, Q. Gong, Z. Gu, Gadolinium-labeled biodegradable dendron–hyaluronic acid hybrid and its subsequent application as a safe and efficient magnetic resonance imaging contrast agent, ACS Appl. Mater. Interfaces 9 (2017) 23508–23519.

[13] T. Lam, P.K. Avti, P. Pouliot, F. Maafi, J.C. Tardif, É. Rhéaume, A. Kakkar, Fabricating water dispersible superparamagnetic iron oxide nanoparticles for biomedical applications through ligand exchange and direct conjugation, Nanomaterials 6 (2016) 100.
[14] B. Sharavanan, K. Sanem, N.L. Yin, F.K. Deborah, J.H. Michael, Robert, Woodward, Timothy G. St Pierre, Judy S. Riffle, Richey M. Davis, Toward design of magnetic nanoparticle clusters stabilized by biocompatible diblock copolymers for T_2-weighted MRI contrast, Langmuir 30 (2014) 1580–1587.
[15] M.R. Carroll, P.P. Huffstetler, W.C. Miles, J.D. Goff, R.M. Davis, J.S. Riffle, St Pierre, the effect of polymer coatings on proton transverse relaxivities of aqueous suspensions of magnetic nanoparticles, Nanotechnology 22 (2011), 325702.
[16] F. Wang, Synthesis of Gadolinium Oxide Based Nanocomposites as Effective Magnetic Resonance Imaging T1 Contrast Agents, Ph.D. Thesis, Hebei University, 2017.
[17] L. Zhang, Y. Liu, D. Yu, N. Zhang, Gadolinium-loaded chitosan nanoparticles as magnetic resonance imaging contrast agents for the diagnosis of tumor, J. Biomed. Nanotechnol. 9 (2013) 863–869.
[18] J.J. Cheng, J. Zhu, X.S. Liu, D.N. He, J.R. Xu, L.M. Wu, Q. Feng, Gadolinium-chitosan nanoparticles as a novel contrast agent for potential use in clinical bowel-targeted MRI: a feasibility study in healthy rats, Acta. Radiol. 53 (2012) 900–907.
[19] L. Faucher, M. Tremblay, J. Lagueux, Y. Gossuin, M.A. Fortin, Rapid synthesis of PEGylated ultrasmall gadolinium oxide nanoparticles for cell labeling and tracking with MRI, ACS Appl. Mater. Interfaces 4 (2012) 4506–4515.
[20] Y. Kobayashi, H. Morimoto, T. Nakagawa, Y. Kubota, K. Gonda, N. Ohuchi, Fabrication of hollow particles composed of silica containing gadolinium compound and magnetic resonance imaging using them, J. Nanostruct. Chem. 3 (2013) 1–6.
[21] S. Marasini, H. Yue, A. Ghazanfari, S.L. Ho, J.A. Park, S. Kim, G.H. Lee, Polyaspartic acid-coated paramagnetic gadolinium oxide nanoparticles as a dual-modal t_1 and t_2 magnetic resonance imaging contrast agent, Appl. Sci. 11 (2021) 8222.
[22] W. Pasanphan, L. Chunkoh, S. Choofong, Magnetic gadolinium-chitosan composite nanoparticles created by radiolytic synthesis, in: 18th International Conferences on Composite Materials, Jeju Island, South Korea, 2011.
[23] S.A. Bon, S.D. Mookhoek, P.J. Colver, H.R. Fischer, S. van der Zwaag, Route to stable non-spherical emulsion droplets, Eur. Polym. J. 43 (2007) 4839–4842.
[24] A. Dufresne, Nanocellulose: a new ageless bionanomaterial, Mater. Today 16 (2013) 220–227.
[25] M. Roman, Toxicity of cellulose nanocrystals: a review, Ind. Biotechnol. 11 (2015) 25–33. .
[26] C. Endes, S. Camarero-Espinosa, S. Mueller, Foster, E.J. Petri-Fink, A.B. Rothen-Rutishauser, M.J.D. Clift, A critical review of the current knowledge regarding the biological impact of nanocellulose, J. Nanobiotechnol. 14 (2016) 1–14.
[27] F.M. Ghorbani, B. Kaffashi, P. Shokrollahi, E. Seyedjafari, A. Ardeshirylajimi, PCL/chitosan/Zn-doped nHA electrospun nanocomposite scaffold promotes adipose derived stem cells adhesion and proliferation, Carbohydr. Polym. 118 (2015) 133–142.
[28] R. Sunasee, U.D. Hemraz, K. Ckless, Cellulose nanocrystals: a versatile nanoplatform for emerging biomedical applications, Expet Opin. Drug Deliv. 13 (2016) 1243–1256.
[29] M. Raza, B. Abu-Jdayil, Cellulose nanocrystals from lignocellulosic feedstock: a review of production technology and surface chemistry modification, Cellulose 29 (2022) 685–722.
[30] F. Whba, F. Mohamed, M.I. Idris, M.S. Yahya, Surface modification of cellulose nanocrystals (CNCs) to form a biocompatible, stable, and hydrophilic substrate for MRI, Appl. Sci. 13 (2023) 6316.
[31] J.H. O'Donnell, D.F. Sangster, Principles of Radiation Chemistry, 1970.
[32] A.M. Abdelghany, E.M. Abdelrazek, S.I. Badr, M.S. Abdel-Aziz, M.A. Morsi, Effect of Gamma-irradiation on biosynthesized gold nanoparticles using Chenopodium murale leaf extract, J. Saudi Chem. Soc. 21 (2017) 528–537.
[33] F. Whba, F. Mohamed, N.R.A.M. Rosli, I.A. Rahman, M.I. Idris, The crystalline structure of gadolinium oxide nanoparticles (Gd_2O_3-NPs) synthesized at different temperatures via X-ray diffraction (XRD) technique, Radiat. Phys. Chem. 179 (2021), 109212.
[34] L. Feng, Z.L. Chen, Research progress on dissolution and functional modification of cellulose in ionic liquids, J. Mol. Liq. 142 (2008) 1–5.
[35] M. Sfiligoj, S. Hribernik, M. Kurečič, A. Urbanek Krajnc, T. Kreže, K. Stana Kleinschek, Cellulose Nanofibres, Surface Properties of Non-conventional Cellulose Fibres, Springer International Publishing, Cham, Switzerland, 2019, pp. 61–71.
[36] F.Y. Cheng, C.H. Su, Y.S. Yang, Characterization of aqueous dispersions of Fe_3O_4 nanoparticles and their biomedical applications, Biomaterials 26 (2005) 729–738.
[37] A. Potthast, S. Radosta, B. Saake, S. Lebioda, T. Heinze, U. Henniges, H. Wetzel, Comparison testing of methods for gel permeation chromatography of cellulose: coming closer to a standard protocol, Cellulose 22 (2015) 1591–1613.
[38] K. Zheng, D. Zhang, D. Zhao, N. Liu, F. Shi, W. Qin, Bright white upconversion emission from Yb^{3+}, Er^{3+}, and Tm^{3+}codoped Gd_2O_3 nanotubes, Phys. Chem. Chem. Phys. 12 (2010) 7620–7625.
[39] D.O. De Castro, J. Bras, A. Gandini, N. Belgacem, Surface grafting of cellulose nanocrystals with natural antimicrobial rosin mixture using a green process, Carbohydrate Polym. 137 (2016) 1–8.
[40] A. Kaboorani, B. Riedl, Surface modification of cellulose nanocrystals (CNC) by a cationic surfactant, Ind. Crop. Prod. 65 (2015) 45–55.
[41] H. Khanjanzadeh, R. Behrooz, N. Bahramifar, W. Gindl-Altmutter, M. Bacher, M. Edler, T. Griesser, Surface chemical functionalization of cellulose nanocrystals by 3-aminopropyltriethoxysilane, Int. J. Biol. Macromol. 106 (2018) 1288–1296.
[42] C.F. Liu, J.L. Ren, F. Xu, J.J. Liu, J.X. Sun, R.C. Sun, Isolation and characterization of cellulose obtained from ultrasonic irradiated sugarcane bagasse, J. Agric. Food Chem. 54 (2006) 5742–5748.
[43] R. Da Silva, M.R. Sierakowski, H.P. Bassani, S.F. Zawadzki, C.L. Pirich, L. Ono, R. A. de Freitas, Hydrophilicity improvement of mercerized bacterial cellulose films by polyethylene glycol graft, Int. J. Biol. Macromol. 86 (2016) 599–605.
[44] L. Goetz, M. Foston, A. Mathew, K. Oksman, A.J. Ragauskas, Poly (methyl vinyl ether-co-maleic acid) – polyethylene glycol nanocomposites cross-linked in situ with cellulose nanowhiskers, Biomacromolecules 11 (2010) 2660–2666.
[45] D.A. McCormick, B.W. Connors, J.W. Lighthall, D.A. Prince, Comparative electrophysiology of pyramidal and sparsely spiny stellate neurons of the neocortex, J. Neurophysiol. 54 (1985) 782–806.
[46] M.Z.A.M. Jamil, F. Mohamed, N.R.A.M. Rosli, I.A. Rahman, M.I. Idris, D. A. Bradley, S.N.M. Mustafa, Effect of gamma irradiation on magnetic gadolinium oxide nanoparticles coated with chitosan (GdNPs-Cs) as contrast agent in magnetic resonance imaging, Radiat. Phys. Chem. 165 (2019), 108407.
[47] D.R. Green, Means to an End: Apoptosis and Other Cell Death Mechanisms, Edisi Ke, Cold Spring Harbor Laboratory Press, 2011.
[48] Z. Liu, X. Liu, Q. Yuan, K. Dong, Li Z. Jiang, J. Ren, X. Qu, Hybrid mesoporous gadolinium oxide nanorods: a platform for multimodal imaging and enhanced insoluble anticancer drug delivery with low systemic toxicity, J. Mater. Chem. 22 (2012) 14982–14990.
[49] Z. Zou, D. He, X. He, K. Wang, X. Yang, Z. Qing, Q. Zhou, Natural gelatin capped mesoporous silica nanoparticles for intracellular acid-triggered drug delivery, Langmuir 29 (2013) 12804–12810.
[50] S. Majeed, S. Shiva Shankar, Rapid, microwave-assisted synthesis of Gd_2O_3 and Eu: Gd_2O_3 nanocrystals: characterization, magnetic, optical and biological studies, J. Mater. Chem. B 2 (2014) 5585–5593.
[51] J.A. Plumb, R. Milroy, S. Kaye, Effects of the ph dependence of 3-(4, 5-dimethylthiazol-2-Yl)-2, 5-diphenyltetrazolium bromide-formazan absorption on chemosensitivity determined by a novel tetrazolium-based assay, Cancer Res. 49 (1989) 4435–4440.
[52] G. Schmalz, Schuster, A. Koch, H. Schweikl, Cytotoxicity of low ph dentin-bonding agents in a dent in barrier test in vitro, J. Endod. 28 (2002) 188–192.
[53] I. ISO, 10993–5: 2009 Biological Evaluation of Medical Devices–Part 5: Tests for in Vitro Cytotoxicity, International Organization for Standardization, Geneva..
[54] M.R. Suryani, H. Ismail, Preparation of curcumin nanoparticles and cellular uptake study on HeLa cells, in: International Conference on Latest Trends in Food, Biological & Ecological Science Proceeding, 2015, pp. 13–17.